Article

Cell Reports

miRNAs that Induce Human Cardiomyocyte Proliferation Converge on the Hippo Pathway

Graphical Abstract

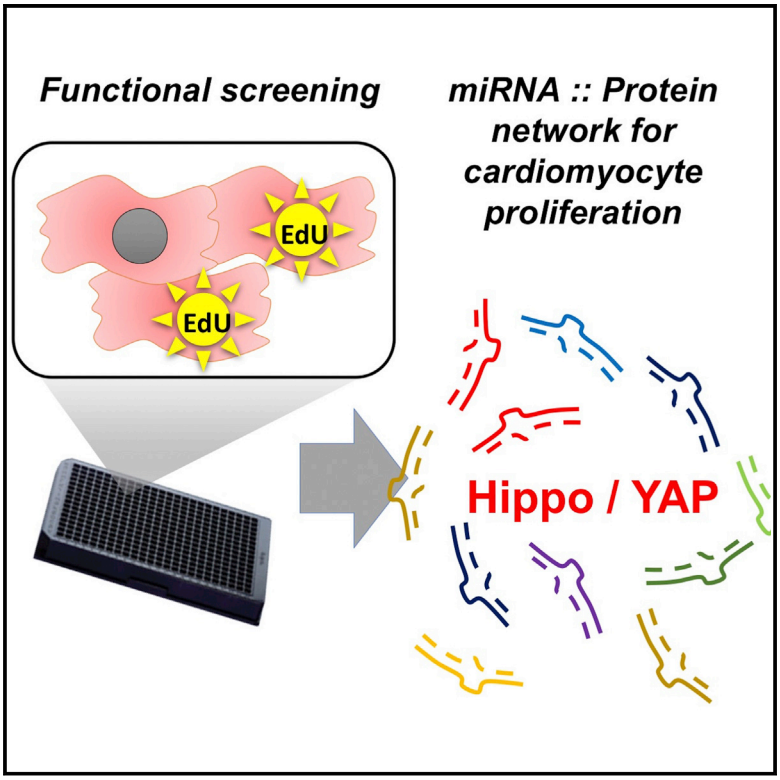

Authors

Marta Diez-Cuñado, Ke Wei, Paul J. Bushway, ..., Shankar Subramaniam, Pilar Ruiz-Lozano, Mark Mercola

Correspondence

pilar@regencor.com (P.R.-L.), mmercola@stanford.edu (M.M.)

In Brief

Diez-Cuñado et al. show that a large set of miRNAs are individually sufficient to promote cell division of immature human cardiomyocytes. Most of these miRNAs act by repressing Hippo and activating YAP, defining Hippo/YAP as a central node controlling cardiomyocyte proliferation and as a promising target to achieve therapeutic cardiac regeneration.

Highlights

- miR'ome screen reveals 96 miRNAs promote human iPSC-derived cardiomyocyte replication
- Most of the miRNAs act by inhibiting Hippo signaling
- The data suggest highly redundant regulation of Hippo components by many miRNAs

Data and Software Availability

GSE111984

Diez-Cuñado et al., 2018, Cell Reports *23*, 2168–2174
May 15, 2018
https://doi.org/10.1016/j.celrep.2018.04.049

CellPress

OPEN ACCESS
CellPress

Cell Reports
Article

miRNAs that Induce Human Cardiomyocyte Proliferation Converge on the Hippo Pathway

Marta Diez-Cuñado,[1] Ke Wei,[1,2] Paul J. Bushway,[1,3] Mano R. Maurya,[3,4] Ranjan Perera,[1] Shankar Subramaniam,[3,4,5] Pilar Ruiz-Lozano,[1,6,7,*] and Mark Mercola[1,3,6,8,*]

[1]Sanford-Burnham-Prebys Medical Discovery Institute, La Jolla, CA 92037, USA
[2]Translational Medical Center for Stem Cell Therapy and Institute for Regenerative Medicine, Shanghai East Hospital, School of Life Sciences and Technology, Tongji University, Shanghai 200092, China
[3]Department of Bioengineering, University of California, San Diego, La Jolla, CA 92093, USA
[4]San Diego Supercomputer Center, University of California, San Diego, La Jolla, CA 92093, USA
[5]Computer Science and Engineering, Cellular and Molecular Medicine, and Graduate Program in Bioinformatics, University of California, San Diego, La Jolla, CA 92093, USA
[6]Stanford Cardiovascular Institute and Department of Medicine, Stanford, CA 94305, USA
[7]Regencor, Inc., Los Altos, CA 92044, USA
[8]Lead Contact
*Correspondence: pilar@regencor.com (P.R.-L.), mmercola@stanford.edu (M.M.)
https://doi.org/10.1016/j.celrep.2018.04.049

SUMMARY

Understanding the mechanisms that control human cardiomyocyte proliferation might be applicable to regenerative medicine. We screened a whole genome collection of human miRNAs, identifying 96 to be capable of increasing proliferation (DNA synthesis and cytokinesis) of human iPSC-derived cardiomyocytes. Chemical screening and computational approaches indicated that most of these miRNAs (67) target different components of the Hippo pathway and that their activity depends on the nuclear translocation of the Hippo transcriptional effector YAP. 53 of the 67 miRNAs are present in human iPSC cardiomyocytes, yet anti-miRNA screening revealed that none are individually essential for basal proliferation of hiPSC cardiomyocytes despite the importance of YAP for proliferation. We propose a model in which multiple endogenous miRNAs redundantly suppress Hippo signaling to sustain the cell cycle of immature cardiomyocytes.

INTRODUCTION

Mammalian cardiomyocytes (CMs) divide during fetal life, but proliferation ceases perinatally (Li et al., 1997). Consequently, the adult myocardium retains only negligible ability for endogenous repair following injury. The control of the CM cell cycle is poorly understood but is considered a possible route to achieve therapeutic regeneration of pediatric and adult hearts (Mercola et al., 2011).

MicroRNAs (miRNAs) are a class of small noncoding RNAs that regulate gene expression at the post-transcriptional level by degrading their target mRNAs and/or inhibiting their translation. miRNAs control nearly all biological processes, including cardiac development, function, and disease (Callis et al., 2009; Chen et al., 2008; Porrello et al., 2011; Sayed and Abdellatif, 2011; van Rooij et al., 2009). Previous studies demonstrated that forced overexpression of certain synthetic miRNAs can promote rodent ventricular CM proliferation (Chen et al., 2013; Eulalio et al., 2012). In particular, miR-590-3p and miR-199-3p can stimulate adult CM proliferation with partial restoration of cardiac mass and function after myocardial infarction, thus revealing the potential of miRNAs in heart regeneration in adult mice (Eulalio et al., 2012). miRNAs and their targets are poorly conserved across species; therefore, the degree to which miRNAs control human CM replication, and the critical pathways they regulate, are unknown. Identifying the basis for human immature CM proliferation could have important implications to understanding certain congenital disorders involving disturbances in myocardial proliferation (Mollova et al., 2013), such as noncompaction and hypoplastic left heart syndrome, and reactivate proliferation therapeutically in quiescent postnatal or adult CMs.

In this study, we performed a large-scale screen of miRNA mimics to define those that are capable of stimulating DNA synthesis and cell division of human induced pluripotent stem cell-derived CMs (hiPSC-CMs). The pro-proliferative miRNAs revealed by this screen overlapped only minimally with those previously shown to stimulate rodent CM proliferation (Eulalio et al., 2012). Computational and functional studies showed that most of the pro-proliferative miRNAs act by targeting the Hippo/YAP pathway, which is an evolutionarily conserved regulator of organ growth and size (Yu and Guan, 2013). Hippo and its cytoplasmic signal transduction pathway suppress cell proliferation by inhibiting the transcriptional activity of YAP/TAZ proteins (Yu and Guan, 2013), and blocking Hippo can reactivate proliferation and induce cardiac regeneration in the adult heart (Lin et al., 2014; von Gise et al., 2012; Xin et al., 2011). In immature induced pluripotent stem cell-derived CMs (iPSC-CMs), we found that mRNAs encoding most Hippo pathway components were recruited to the RNA-induced silencing complex (RISC), implicating tight miRNA control of the pathway. Moreover, of the 67 Hippo pathway regulating miRNAs identified herein, two

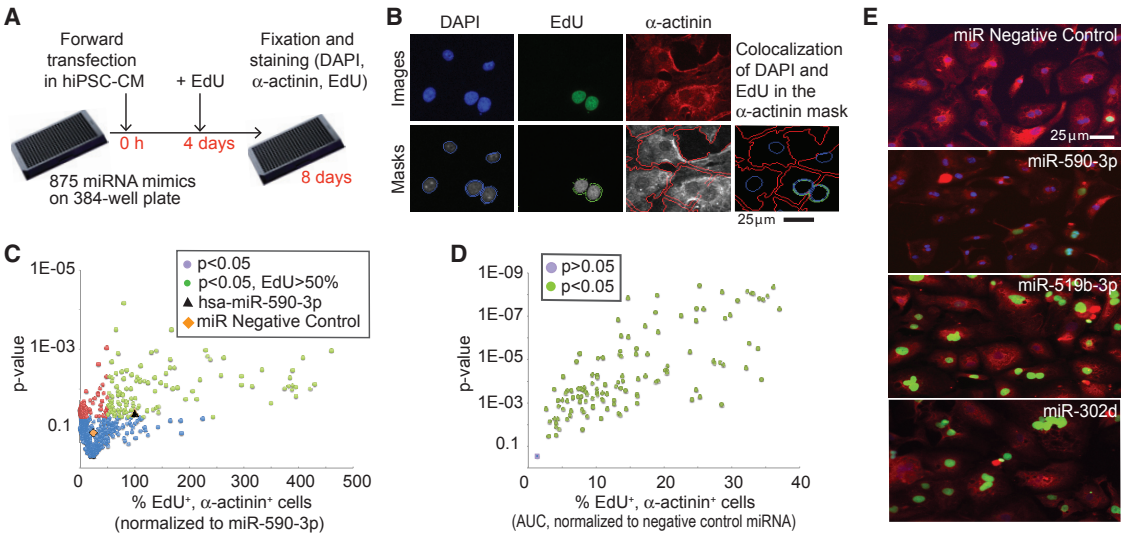

Figure 1. Screen for miRNAs that Regulate hiPSC-CM DNA Synthesis

(A) Experimental design of the primary screen to evaluate the effect of synthetic human miRNA mimics on DNA synthesis by EdU incorporation.

(B) Images and image masks (outlines are colored) for EdU, α-actinin, and DAPI signals. Cardiomyocytes were scored as proliferative if positive for α-actinin and EdU within the DAPI mask.

(C) Volcano plot of the primary screen results. The incidence of EdU incorporation (as a percentage) is normalized to the miR-590-3p (positive control) value. The thresholds for hit selection were $p < 0.05$ (Benjamini FDR < 0.13) and EdU incorporation > 50% (represented in green).

(D) Volcano plot of the confirmatory screen results. The incidence of EdU incorporation (as a percentage) is calculated as an area under the curve (AUC) of five doses for the individual miRNAs normalized to the value for the negative control miRNA.

(E) Immunostaining examples from the primary screen showing the expression of EdU (green), α-actinin (red), and DAPI (blue) in hiPSC-CMs after transfection of miRNA negative control and three miRNAs that promote hiPSC-CM proliferation.

(miR302-367 and miR-17-92) have been shown to induce cardiac regeneration (Tian et al., 2015). None of the pro-proliferation miRNAs were found to be essential for iPSC-CM cell division, although more than 50 are present in immature CMs and YAP is required for their basal rate of proliferation. We speculate that this apparent functional redundancy indicates that multiple endogenous miRNAs suppress Hippo and activate YAP to sustain the proliferative state of immature CMs.

RESULTS

Multiple miRNAs Stimulate hiPSC-CM Cell Division

To identify miRNAs that control the proliferation of human CMs, we screened a library of 875 synthetic human miRNA mimics for the ability to induce hiPSC-CMs to proliferate. The overall approach included the independent functional evaluation of DNA duplication (Figure 1) and cytokinesis (Figure 2).

For the primary screen (Figure 1A), synthetic miRNA mimics were transferred to plates previously seeded with hiPSC-CMs for forward transfection. After 8 days, the cells were co-stained for the CM marker sarcomeric α-actinin and the nucleoside analog of thymidine 5-ethynyl-2′-deoxyuridine (EdU), which is incorporated into newly synthesized DNA. The incidence of double-positive EdU$^+$, α-actinin$^+$ cells was quantified using an automated algorithm (Figure 1B) (Supplemental Experimental Procedures). The screen results are depicted as a volcano plot relating the activities (x axis) of the individual miRNAs and the corresponding p values (y axis) (Figure 1C). 128 miRNA mimics increased the incidence of EdU incorporation in hiPSC-CMs above a threshold of >50% of that achieved by the positive control miRNA, hsa-miR-590-3p (Eulalio et al., 2012), which was assigned a value of 100% ($p < 0.05$; Benjamini false discovery rate [FDR] < 0.13). Rescreening through a dose range (20 to 1.25 nM) yielded 127 miRNAs as statistically significant enhancers of CM DNA duplication ($p < 0.05$; Benjamini FDR < 0.03) (Figures 1D and 1E; Table S1).

A secondary assay was developed to identify those miRNAs that promoted cytokinesis, in addition to stimulating CM DNA synthesis. For that purpose, we adapted a carboxyfluorescein succinimidyl ester (CFSE) dilution method previously used in flow cytometry (Figure 2A) (Filby et al., 2015). In this assay, the fluorescent intensity of cytoplasmic labeling with CFSE is progressively halved following each cell division and quantified in the cytoplasm of α-actinin$^+$ hiPSC-CMs, creating a bona fide index of the duplication rate (see Experimental Procedures). Using this assay to filter the primary screen hits also removed any miRNAs that promoted endo-reduplication or polyploidization, both of which occur in CMs. Of the 127 miRNA mimics selected, 96 significantly increased cytokinesis over the basal rate achieved with an inert negative control miRNA ($p < 0.05$; Benjamini FDR < 0.07) (Figure 2B). To verify that the effect was caused by cell division, nocodazole, a microtubule polymerization inhibitor that blocks cytokinesis, eliminated all miRNA-induced cytokinesis, demonstrating the specific effect of these miRNAs for cell division (Figure 2C; summarized in Figure 2D).

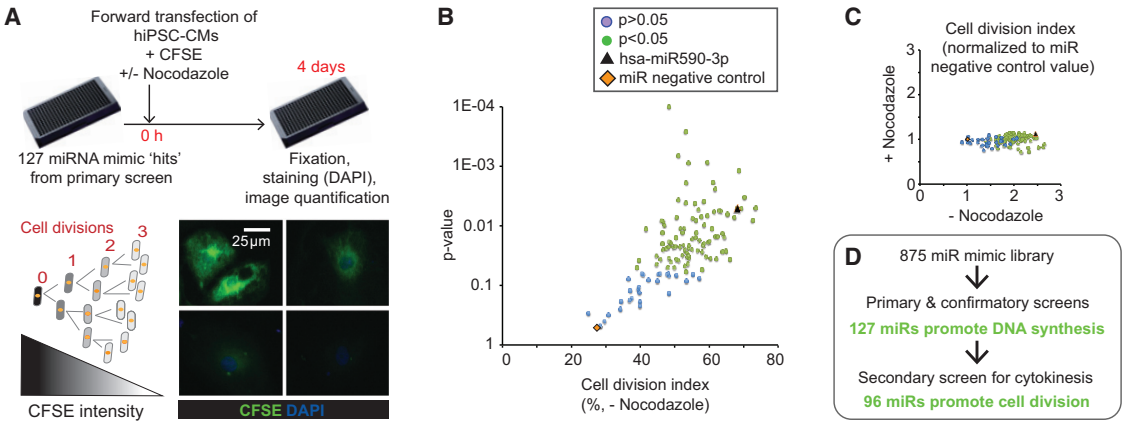

Figure 2. Screen for miRNAs that Regulate hiPSC-CM Cell Division

(A) Experimental design of the secondary assay to evaluate cytokinesis. The cell division index reflects the dilution of cytoplasmic CFSE fluorescence (see Experimental Procedures). Representative images of cells are shown.

(B) Volcano plot correlating cell division index to the p value for the 127 miRNAs that increased the incidence of EdU incorporation.

(C) Effect of the microtubule polymerization inhibitor nocodazole on the cell division index normalized to that of the negative control miRNA.

(D) Summary of the primary and secondary screen results. From a library of human miRNA mimics (875), 96 miRNAs promoted DNA synthesis and cytokinesis in hiPSC-CMs.

Proliferation-Inducing miRNAs Converge on a Limited Set of Target Pathways

miRSystem software (Lu et al., 2012) predicted that the 96 pro-proliferative miRNAs target 15,776 genes, out of which 12,953 are expressed in hiPSC-CMs (CM expressed [CE]). Using Database for Annotation, Visualization and Integrated Discovery (DAVID) Bioinformatics Resources (Huang et al., 2009a, 2009b), 4,776 of these CE candidate target genes were mapped onto Kyoto Encyclopedia of Genes and Genomes (KEGG) pathways, resulting in 32 possible signaling pathways with Benjamini FDR < 0.05 (Figure 3A; Table S3A).

To focus on proteins and pathways that are relevant to CM proliferation, we rescreened the EdU proliferation assay against 160 well-characterized small molecule kinase inhibitors, each with known target space (Gao et al., 2013). Because kinases are prominent intracellular signaling nodes, a kinase inhibitor screen would discriminate relevant from irrelevant signaling pathways. The screen yielded 103 inactive, 36 inhibitory, and 21 inducing compounds (Figure S2; Table S2). Because miRNAs act by suppressing translation of their mRNA targets, the kinases that are uniquely inhibited by the inactive and inhibitory compounds (targeting 71 and 43 proteins, respectively) are unlikely to be targets of the pro-proliferative miRNAs and therefore were removed from the protein set (Figure 3A). The 54 protein kinases targeted by the inducer compounds were retained (Figure 3A). This functional screening approach to KEGG pathway enrichment reduced the number of candidate signaling pathways targeted by the miRNAs from 32 to 8 (Benjamini FDR < 0.05), namely, thyroid hormone (TH), phosphatidylinositol (PI), estrogen (E2), protein kinase G (cGMP)-PKG, adrenergic, Wnt, Notch, and Hippo pathways (Figure 3A; see Table S3B for the complete list of pathways). Previous work has shown functional interconnectedness within these key pathways: Hippo/YAP is regulated by adrenergic signaling (Yu et al., 2012). Suppression of Hippo signaling (which causes nuclear translocation and activation of YAP) (Figure 3B) promotes CM proliferation partly by de-repressing Wnt (Heallen et al., 2011) and activating Notch (Campa et al., 2008; Collesi et al., 2008; Irvine, 2012) pathways. Therefore, we focused our subsequent target analysis of the screen data on Hippo signaling.

Small interfering RNA (siRNA) knockdown of YAP decreased the incidence of EdU incorporation. Conversely, siRNA knockdown of LATS1 (a Hippo pathway component and a negative regulator of YAP) increased EdU incorporation in hiPSC-CMs (Figure 3C), suggesting that Hippo/YAP is an important regulator of the basal rate of proliferation.

We evaluated whether the individual miRNAs modified the subcellular localization of YAP. 84 of the 96 pro-proliferative miRNAs increased the ratio of nuclear to cytoplasmic localized YAP (Figure 3D), providing evidence that these miRNAs act on or proximal to the Hippo/YAP pathway. Furthermore, siRNA against YAP blocked the ability of 70 of the 96 miRNAs to stimulate EdU incorporation in hiPSC-CMs (Figure 3E; validation of the YAP knockdown is shown in Figure S3). Altogether, 67 of the 96 pro-proliferative miRNAs increased nuclear localization of YAP and depended on YAP for their proliferation-inducing activity (Figure 3F; Table S3C).

Possible Redundant Control of Hippo by Endogenous miRNAs

The preceding gain-of-function experiments revealed 67 miRNAs that can stimulate hiPSC-CM proliferation in a YAP-dependent manner. Because siRNA against YAP decreased the basal rate of hiPSC-CM proliferation (Figure 3C), we asked whether endogenous miRNAs might sustain proliferation. Of the 67 YAP-dependent pro-proliferation miRNAs, 53 are expressed in hiPSC-CMs as shown by RNA sequencing (RNA-seq) profiling and were examined by selective knockdown with locked nucleic acid (LNA) antisense miRNAs (anti-miRs). None of the individually transfected 53 anti-miRs blunted EdU incorporation (Figure 4A;

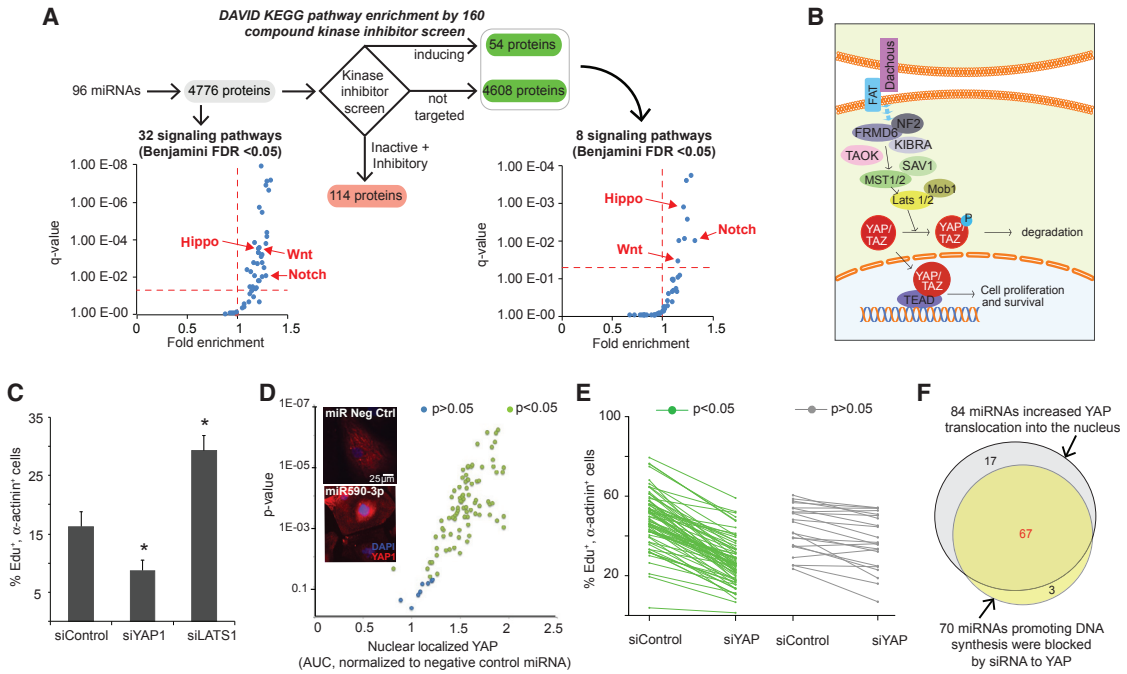

Figure 3. miRNAs Promoting hiPSC-CM Proliferation by Regulating the Hippo Pathway

(A) Summary of the functional enrichment of the computationally predicted and cardiac-expressed targets of miRNAs. Based on a screen of 160 small molecule kinase inhibitors (see text, Figure S2, and Table S2), 114 unique protein targets of inactive and inhibitory compounds were excluded from the DAVID-based KEGG pathway set, decreasing the total number of candidate protein targets from 4,776 to 4,662. The number of candidate signaling pathways (Benjamini FDR < 0.05) decreased from 32 to 8 (see Tables S3A and S3B for complete lists of pathways). Fold enrichment is defined in Supplemental Experimental Procedures.

(B) Schematic of the Hippo signaling pathway.

(C) Effect of siRNAs against YAP and LATS1 on the incidence (as a percentage) of EdU$^+$, α-actinin$^+$ cells. Error bars, SD; n = 3.

(D) Volcano plot of the effect of 96 miRNA mimics transfected on nuclear localization of YAP. Examples of immunostaining of YAP (red) and DAPI (blue) in hiPSC-CMs transfected with miRNA negative control and miR-590-3p.

(E) Effect of siRNA to YAP relative to control siRNA on the incidence (as a percentage) of EdU$^+$, α-actinin$^+$ cells. Graphs show miRNAs that were significantly ($p < 0.05$) blocked (left, green) or not blocked (right, gray) by siRNA to YAP relative to control (see Table S3C for the complete dataset).

(F) Venn diagram showing the total number of proliferation-inducing miRNAs (67) that increased the nuclear translocation of YAP (D) and whose activity depends on YAP (E).

Table S4A) relative to that observed either upon transfection of a negative control LNA antisense RNA (selected for lack of homology to any miRNA; see Experimental Procedures) or to mock transfection conditions (data not shown). However, one anti-miR caused an ~2× increase that was at the threshold (Benjamini FDR < 0.05 of significance) (Figure 1D; Table S1). None of the anti-miRs diminished the basal ratio of nuclear-to-cytoplasmic localized YAP (Figure S4). Altogether, these data suggest that none of the miRNAs are individually required to sustain the level of nuclear YAP or the basal rate of proliferation.

The computationally predicted targets of the 67 miRNAs, including the 53 expressed in hiPSC-CMs (asterisks in Figure 4B), indicate a remarkable degree of redundancy among the miRNAs for components of the Hippo pathway. Every protein of the core pathway is predicted to be targeted by multiple miRNAs expressed in hiPSC-CMs, with a bias for inhibiting proteins that would activate YAP (indicated by green in the heatmap representation), and each miRNA is predicted to target multiple components (Figure 4B). For example, miR-520d-3p predicted targets are FAT2, FAT4, FRMD6, NF2, TAOK1, TAOK2, LATS2, and TEAD1; miR-590-3p predicted targets are FAT1, FAT3, FRMD6, MOBKL1A, YAP, and TEAD; and in the case of miR-17 family members, 14 proteins from the Hippo pathway are repressed by these miRNAs (FAT2, FAT3, FAT4, FRMD6, NF2, TAOK1, TAOK2, TAOK3, MST2, SAV1, LATS2, MOBKL1A, TEAD1, and TEAD3).

Finally, we asked experimentally whether core Hippo pathway components are under control by endogenous miRNAs. miRNAs suppress protein production by recruiting target mRNAs to the RISC, where they associate with Argonaute (Ago) proteins. Argonaute immunopurification (AgoIP) followed by RNA-seq allows the unbiased, comprehensive identification of miRNA target genes (Matkovich et al., 2011). AgoIP/RNA-seq of normal, untransfected hiPSC-CMs showed that mRNAs encoding 22 of 25 core Hippo pathway components are present in RISC (Figure 4C), using a Benjamini FDR cutoff of 0.05 to call significant regions. See Table S4B for the complete dataset of the peaks enriched by AgoIP relative to control immunoglobulin G (IgG) immunopurification. Most transcripts exhibited multiple AgoIP/RNA-seq peaks (relative to control IgG), indicating multiple sites of miRNA:mRNA interaction.

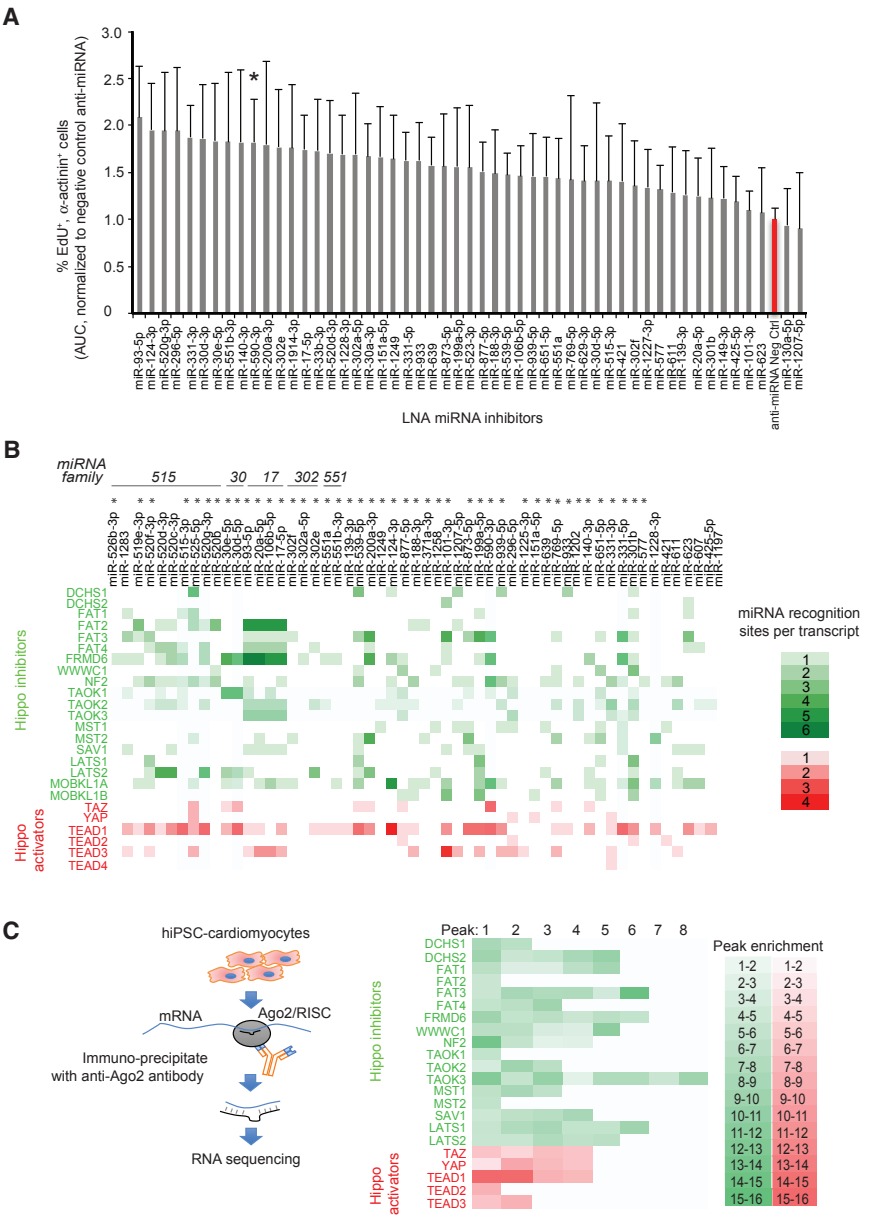

Figure 4. miRNAs Target Hippo Pathway Genes

(A) Anti-miRNA screen for hiPSC-CM proliferation. Incidence (as a percentage) of EdU$^+$, α-actinin$^+$ cells calculated as area under the curve (AUC) of three doses of the anti-miRs corresponding to the 53 endogenously expressed proliferation miRNAs and normalized to the value for the negative control anti-miRNA. Error bars, SD; n = 3.

(B) The computationally predicted pathway (miRSystem) components targeted by the 67 proliferation-inducing miRNAs that act through YAP (Figure 3F). The heatmap representation indicates the number of recognition sequences in the mRNA transcript (scale). Green signifies genes that inhibit nuclear translocation of YAP and inhibit cell proliferation; red signifies genes that promote cell proliferation. The asterisks indicate miRNAs expressed in hiPSC-CMs.

(C) Scheme of the AgoIP/RNA sequencing experiment (left). Results of AgoIP/RNA-seq analysis showing the Hippo pathway core genes (right). The columns indicate individual peaks enriched by AgoIP relative to control IgG immunopurification oriented from by chromosome start and end positions (see Table S4A for the RNA-seq dataset). The heatmap color-coding represents fold enrichment by AgoIP (see Supplemental Experimental Procedures). Green and red are as in (B).

DISCUSSION

Our initial functional screen revealed, upon overexpression, 96 synthetic human miRNAs that can promote DNA synthesis and cytokinesis in hiPSC-CMs. To identify pathways responsible for mediating the proliferative effect of the miRNAs, we filtered the computationally predicted target set by removing kinases that are uniquely inhibited by small molecule kinase inhibitors that do not induce proliferation (Figure 3A; Table S2). Although this decreased the number of predicted proteins in the DAVID KEGG database by only 114 (from 4,776 to 4,662), it had a disproportionate effect on signaling pathways (decreasing the number from 32 to 8) because of the prevalence of kinases as signaling mediators (Figure 3A; Table S3). In addition to Hippo/YAP, Wnt and Notch pathways were represented. Suppression of Hippo signaling de-represses Wnt/β-catenin target genes that contribute to CM proliferation (Heallen et al., 2011). Similarly, suppression of Hippo is a potent activator of Notch signaling (Irvine, 2012), which has a well-defined role in sustaining immature CM proliferation (Campa et al., 2008; Collesi et al., 2008), together indicating that Wnt and Notch act downstream of Hippo. In contrast, adrenergic signaling has been reported to act upstream to regulate Hippo/YAP (Yu et al., 2012). Other pathways were TH, PI, E2, and cGMP-PKG, which have documented roles in hypertrophy and apoptosis (Francis, 2010; Matsui et al., 2003; Ojamaa, 2010; van Eickels et al., 2001). Because most miRNAs (84/96) induced nuclear translocation of YAP, we focused our efforts on Hippo/YAP. An unexpected finding was that most these miRNAs (67/84) required YAP for their proliferative activity.

Although many of the miRNAs that regulate Hippo are expressed in hiPSC-CMs (53), none were found to be essential to sustain the basal rate of proliferation when knocked down individually (Figure 4A). This contrasts with knockdown of YAP, which decreased basal iPSC-CM proliferation (Figure 3C). Furthermore, none of the individual LNA anti-miRNAs blocked YAP translocation (Figure S4), indicating that YAP was still active in the presence of the anti-miRNAs. From these data, we infer that multiple endogenous miRNAs might redundantly converge

on Hippo signaling to activate YAP and robustly sustain proliferation.

A limitation of this work, common to overexpression studies, is that transfected miRNAs or siRNAs can distort the profile of endogenous miRNAs loaded into RISC (Khan et al., 2009), potentially generating false negatives and positives. In addition, it is not technically feasible to simultaneously attenuate all predicted Hippo-targeting miRNAs, thus preventing direct experimental confirmation of the model that endogenous miRNAs redundantly suppress the Hippo pathway. Nonetheless, the idea of redundant regulation is corroborated by computational data predicting that nearly all components of the pathway are targeted by the proliferation-inducing miRNAs (Figure 4B) and the experimental finding that mRNAs encoding most Hippo/YAP pathway components in immature iPSC-CMs are normally present in RISC (Figure 4C; Table S4B). The concept that multiple miRNAs redundantly suppress a common biological process to stabilize a system against physiological challenge has been substantiated by mathematical modeling (Lai et al., 2016). In addition, our data predict that both positive and negative regulators of YAP are under miRNA control and, in some cases, by the same miRNA or miRNAs with similar seed sequences (Figures 4B and 4C). Other biological examples in which miRNAs may buffer pathway activity by simultaneously dampening expression of positive and negative regulators include the miR-26 family, which targets both pro- and anti-tumorigenic targets, and miR-143/145, which both positively and negatively regulate transcription factors involved in smooth muscle proliferation and differentiation (Mendell and Olson, 2012). In both miR-26 and miR-143/145, cell context dictates which phenotype predominates.

In summary, we identified 96 miRNAs capable of promoting hiPSC-CM proliferation upon overexpression. There is only minimal overlap between these miRNAs acting in human CMs and those from a similar screen performed using rodent CMs, even when comparing miRNAs that are evolutionarily conserved (Figure S1). A lack of correlation is consistent with the evolutionary divergence of the mRNA sequences recognized by miRNAs (Berezikov, 2011). Several murine studies have suggested that inhibition of Hippo can reactivate proliferation and induce cardiac regeneration in the adult heart (Lin et al., 2014; von Gise et al., 2012; Xin et al., 2011), including by overexpression of two miRNAs (miR-302-367 and miR-17-92) (Tian et al., 2015). This concept is relevant to both adult and pediatric disease. Our data indicate that the same process might occur in humans, although the miRNAs will likely differ between species.

EXPERIMENTAL PROCEDURES

Further details and an outline of resources used in this work can be found in Supplemental Experimental Procedures.

MicroRNA Screening and Primary and Secondary Analysis

hiPSC-CMs were purchased from Cellular Dynamics International (CDI). Cells were plated on 384-well plates coated with gelatin and forward transfected with miRNA mimics (Applied Biosystems) using RNAiMAX (Life Technologies) in triplicate, with 10 nM each miRNA. For primary screening, the cells were assayed for EdU incorporation. Image acquisition was performed using an automated, high-content screening fluorescent microscope (InCell Analyzer 1000, GE Healthcare) at 10× magnification. 16 images were acquired per wavelength, well, and replicate, corresponding to approximately 4,000 cells analyzed per condition. Image analysis was performed using custom algorithms written using GE Healthcare Software Developer Toolbox v.1.9.

For secondary screening, cells were cultured in the presence of 5 μM CellTrace CFSE (Life Technologies) before transfection and then cultured for another 4 days and imaged. Imaging was performed using a high-content fluorescent microscope (IC200-KIC, Vala Sciences) and analyzed using CyteSeer software (Vala Sciences). CE mRNAs and miRNAs were as described (SuperSeries [mRNA + miRNA], GSE60293; mRNA expression array, GSE60291; and miRNA-seq, GSE60292).

Kinase Inhibitor Screen for EdU Incorporation

Cells were treated with the InhibitorSelect 384-well Protein Kinase Inhibitor Library (EMD Millipore) using 4 replicates for each compound and following the same protocol as for the primary screen. Final concentration of compounds ranged from 0.5 to 5 μM (depending on the original concentration in the master plate from EMD Millipore), and DMSO was used as internal control. Fluorescent immunochemistry, image acquisition, and analysis were performed as for the primary screen. Targets of the kinase inhibitors are published (Gao et al., 2013).

siRNAs and Transfection of hiPSC-CMs

To evaluate the effect of the Hippo signaling pathway on hiPSC-CM proliferation, cells were plated and cultured as previously described in the 384-well plate format. One week after plating, they were forward transfected with 50 nM siRNA negative control, siRNA against YAP (ON-TARGETplus SMARTpool siRNA/YAP1, Dharmacon/GE Healthcare), or siRNA against LATS1 (ON-TARGETplus/LATS1, Dharmacon/GE Healthcare) using DharmaFECT 1 transfection reagent (Dharmacon). The target sequence of siYAP is 5′-GCACCUAUCACUCUCGAGA-3′. The target sequence of siLATS1 is 5′-GGUGAAGUCUGUCUAGCAA-3′. After 4 days of transfection, 10 μM EdU was added into the media and, after 4 days incubation, cells were fixed and processed for fluorescent immunochemistry, image acquisition, and analysis as described earlier.

Statistics

Data are presented as mean ± SD of the mean. Unpaired Student's t test was performed to determine statistical differences. The Benjamini-Hochberg method was used to determine the FDR.

DATA AND SOFTWARE AVAILABILITY

The accession number for the miRNA profiling data reported in this paper is GEO: GSE111984.

SUPPLEMENTAL INFORMATION

Supplemental Information includes Supplemental Experimental Procedures, four figures, and four tables and can be found with this article online at https://doi.org/10.1016/j.celrep.2018.04.049.

ACKNOWLEDGMENTS

We thank Ximena Garate and Agustin Rojas-Munoz for providing AgoIP/sequencing data, Matthew Greenhaw for the computational analysis of Figure 4C, and Ulrich Broeckel for providing an hiPSC-CM transcriptome dataset. We acknowledge grant support from the NIH (1R01HL132225, 1R01HL130840, 1R01HL128072, and 1R01HL113601 to M.M.; R01HL065484 and R01HL086879 to P.R.-L.; and R01HL106579 and R01HL108735 to S.S.), National Science Foundation (NSF) collaborative grant STC-0939370, and the Fondation Leducq (Shapeheart). M.D.-C. was a California Institute for Regenerative Medicine (CIRM TG2-0116) postdoctoral fellow. Core facilities were supported by the NIH (5P30AR061303 and 5P30CA030199).

AUTHOR CONTRIBUTIONS

M.D.-C. was responsible for the conceptualization, analysis, experimentation, and writing; K.W. performed analysis; P.J.B. was responsible for software and

methodology; M.R.M. performed informatics analysis and data curation; R.P. provided technical resources, funding, and supervision; S.S., P.R.-L., and M.M. were responsible for conceptualization, supervision, writing and funding. All authors edited the manuscript.

DECLARATION OF INTERESTS

The authors declare no competing interests.

Received: February 17, 2017
Revised: July 28, 2017
Accepted: April 12, 2018
Published: May 15, 2018

REFERENCES

Berezikov, E. (2011). Evolution of microRNA diversity and regulation in animals. Nat. Rev. Genet. *12*, 846–860.

Callis, T.E., Pandya, K., Seok, H.Y., Tang, R.H., Tatsuguchi, M., Huang, Z.P., Chen, J.F., Deng, Z., Gunn, B., Shumate, J., et al. (2009). MicroRNA-208a is a regulator of cardiac hypertrophy and conduction in mice. J. Clin. Invest. *119*, 2772–2786.

Campa, V.M., Gutiérrez-Lanza, R., Cerignoli, F., Díaz-Trelles, R., Nelson, B., Tsuji, T., Barcova, M., Jiang, W., and Mercola, M. (2008). Notch activates cell cycle reentry and progression in quiescent cardiomyocytes. J. Cell Biol. *183*, 129–141.

Chen, J.F., Murchison, E.P., Tang, R., Callis, T.E., Tatsuguchi, M., Deng, Z., Rojas, M., Hammond, S.M., Schneider, M.D., Selzman, C.H., et al. (2008). Targeted deletion of Dicer in the heart leads to dilated cardiomyopathy and heart failure. Proc. Natl. Acad. Sci. USA *105*, 2111–2116.

Chen, J., Huang, Z.P., Seok, H.Y., Ding, J., Kataoka, M., Zhang, Z., Hu, X., Wang, G., Lin, Z., Wang, S., et al. (2013). miR-17-92 cluster is required for and sufficient to induce cardiomyocyte proliferation in postnatal and adult hearts. Circ. Res. *112*, 1557–1566.

Collesi, C., Zentilin, L., Sinagra, G., and Giacca, M. (2008). Notch1 signaling stimulates proliferation of immature cardiomyocytes. J. Cell Biol. *183*, 117–128.

Eulalio, A., Mano, M., Dal Ferro, M., Zentilin, L., Sinagra, G., Zacchigna, S., and Giacca, M. (2012). Functional screening identifies miRNAs inducing cardiac regeneration. Nature *492*, 376–381.

Filby, A., Begum, J., Jalal, M., and Day, W. (2015). Appraising the suitability of succinimidyl and lipophilic fluorescent dyes to track proliferation in non-quiescent cells by dye dilution. Methods *82*, 29–37.

Francis, S.H. (2010). The role of cGMP-dependent protein kinase in controlling cardiomyocyte cGMP. Circ. Res. *107*, 1164–1166.

Gao, Y., Davies, S.P., Augustin, M., Woodward, A., Patel, U.A., Kovelman, R., and Harvey, K.J. (2013). A broad activity screen in support of a chemogenomic map for kinase signalling research and drug discovery. Biochem. J. *451*, 313–328.

Heallen, T., Zhang, M., Wang, J., Bonilla-Claudio, M., Klysik, E., Johnson, R.L., and Martin, J.F. (2011). Hippo pathway inhibits Wnt signaling to restrain cardiomyocyte proliferation and heart size. Science *332*, 458–461.

Huang, D.W., Sherman, B.T., and Lempicki, R.A. (2009a). Bioinformatics enrichment tools: paths toward the comprehensive functional analysis of large gene lists. Nucleic Acids Res. *37*, 1–13.

Huang, D.W., Sherman, B.T., and Lempicki, R.A. (2009b). Systematic and integrative analysis of large gene lists using DAVID bioinformatics resources. Nat. Protoc. *4*, 44–57.

Irvine, K.D. (2012). Integration of intercellular signaling through the Hippo pathway. Semin. Cell Dev. Biol. *23*, 812–817.

Khan, A.A., Betel, D., Miller, M.L., Sander, C., Leslie, C.S., and Marks, D.S. (2009). Transfection of small RNAs globally perturbs gene regulation by endogenous microRNAs. Nat. Biotechnol. *27*, 549–555.

Lai, X., Wolkenhauer, O., and Vera, J. (2016). Understanding microRNA-mediated gene regulatory networks through mathematical modelling. Nucleic Acids Res. *44*, 6019–6035.

Li, F., Wang, X., Bunger, P.C., and Gerdes, A.M. (1997). Formation of binucleated cardiac myocytes in rat heart: I. Role of actin-myosin contractile ring. J. Mol. Cell. Cardiol. *29*, 1541–1551.

Lin, Z., von Gise, A., Zhou, P., Gu, F., Ma, Q., Jiang, J., Yau, A.L., Buck, J.N., Gouin, K.A., van Gorp, P.R., et al. (2014). Cardiac-specific YAP activation improves cardiac function and survival in an experimental murine MI model. Circ. Res. *115*, 354–363.

Lu, T.P., Lee, C.Y., Tsai, M.H., Chiu, Y.C., Hsiao, C.K., Lai, L.C., and Chuang, E.Y. (2012). miRSystem: an integrated system for characterizing enriched functions and pathways of microRNA targets. PLoS ONE *7*, e42390.

Matkovich, S.J., Van Booven, D.J., Eschenbacher, W.H., and Dorn, G.W., 2nd. (2011). RISC RNA sequencing for context-specific identification of *in vivo* microRNA targets. Circ. Res. *108*, 18–26.

Matsui, T., Nagoshi, T., and Rosenzweig, A. (2003). Akt and PI 3-kinase signaling in cardiomyocyte hypertrophy and survival. Cell Cycle *2*, 220–223.

Mendell, J.T., and Olson, E.N. (2012). MicroRNAs in stress signaling and human disease. Cell *148*, 1172–1187.

Mercola, M., Ruiz-Lozano, P., and Schneider, M.D. (2011). Cardiac muscle regeneration: lessons from development. Genes Dev. *25*, 299–309.

Mollova, M., Bersell, K., Walsh, S., Savla, J., Das, L.T., Park, S.Y., Silberstein, L.E., Dos Remedios, C.G., Graham, D., Colan, S., and Kühn, B. (2013). Cardiomyocyte proliferation contributes to heart growth in young humans. Proc. Natl. Acad. Sci. USA *110*, 1446–1451.

Ojamaa, K. (2010). Signaling mechanisms in thyroid hormone-induced cardiac hypertrophy. Vascul. Pharmacol. *52*, 113–119.

Porrello, E.R., Johnson, B.A., Aurora, A.B., Simpson, E., Nam, Y.J., Matkovich, S.J., Dorn, G.W., 2nd, van Rooij, E., and Olson, E.N. (2011). miR-15 family regulates postnatal mitotic arrest of cardiomyocytes. Circ. Res. *109*, 670–679.

Sayed, D., and Abdellatif, M. (2011). MicroRNAs in development and disease. Physiol. Rev. *91*, 827–887.

Tian, Y., Liu, Y., Wang, T., Zhou, N., Kong, J., Chen, L., Snitow, M., Morley, M., Li, D., Petrenko, N., et al. (2015). A microRNA-Hippo pathway that promotes cardiomyocyte proliferation and cardiac regeneration in mice. Sci. Transl. Med. *7*, 279ra38.

van Eickels, M., Grohé, C., Cleutjens, J.P., Janssen, B.J., Wellens, H.J., and Doevendans, P.A. (2001). 17beta-estradiol attenuates the development of pressure-overload hypertrophy. Circulation *104*, 1419–1423.

van Rooij, E., Quiat, D., Johnson, B.A., Sutherland, L.B., Qi, X., Richardson, J.A., Kelm, R.J., Jr., and Olson, E.N. (2009). A family of microRNAs encoded by myosin genes governs myosin expression and muscle performance. Dev. Cell *17*, 662–673.

von Gise, A., Lin, Z., Schlegelmilch, K., Honor, L.B., Pan, G.M., Buck, J.N., Ma, Q., Ishiwata, T., Zhou, B., Camargo, F.D., and Pu, W.T. (2012). YAP1, the nuclear target of Hippo signaling, stimulates heart growth through cardiomyocyte proliferation but not hypertrophy. Proc. Natl. Acad. Sci. USA *109*, 2394–2399.

Xin, M., Kim, Y., Sutherland, L.B., Qi, X., McAnally, J., Schwartz, R.J., Richardson, J.A., Bassel-Duby, R., and Olson, E.N. (2011). Regulation of insulin-like growth factor signaling by Yap governs cardiomyocyte proliferation and embryonic heart size. Sci. Signal. *4*, ra70.

Yu, F.X., and Guan, K.L. (2013). The Hippo pathway: regulators and regulations. Genes Dev. *27*, 355–371.

Yu, F.X., Zhao, B., Panupinthu, N., Jewell, J.L., Lian, I., Wang, L.H., Zhao, J., Yuan, H., Tumaneng, K., Li, H., et al. (2012). Regulation of the Hippo-YAP pathway by G-protein-coupled receptor signaling. Cell *150*, 780–791.